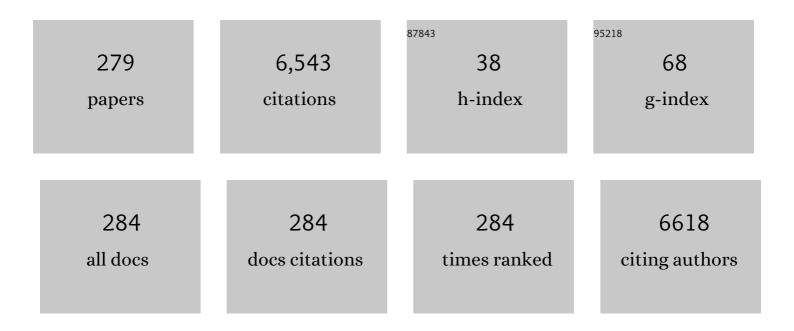
List of Publications by Year in descending order

Source: https://exaly.com/author-pdf/5546409/publications.pdf Version: 2024-02-01



FENC WANC

#	Article	IF	CITATIONS
1	Carbon Nanotubes with Titanium Nitride as a Lowâ€Cost Counterâ€Electrode Material for Dyeâ€Sensitized Solar Cells. Angewandte Chemie - International Edition, 2010, 49, 3653-3656.	7.2	554
2	Rational design of donor-ï€-acceptor conjugated microporous polymers for photocatalytic hydrogen production. Applied Catalysis B: Environmental, 2018, 228, 1-9.	10.8	215
3	Dibenzothiophene Dioxide Based Conjugated Microporous Polymers for Visible-Light-Driven Hydrogen Production. ACS Catalysis, 2018, 8, 8590-8596.	5.5	202
4	Porous carbons derived from hypercrosslinked porous polymers for gas adsorption and energy storage. Carbon, 2017, 114, 608-618.	5.4	170
5	Conjugated Microporous Polymers with Tunable Electronic Structure for High-Performance Potassium-Ion Batteries. ACS Nano, 2019, 13, 745-754.	7.3	162
6	Toward High Performance Thiopheneâ€Containing Conjugated Microporous Polymer Anodes for Lithiumâ€ion Batteries through Structure Design. Advanced Functional Materials, 2018, 28, 1705432.	7.8	162
7	Conjugated Fluorene and Silole Copolymers:  Synthesis, Characterization, Electronic Transition, Light Emission, Photovoltaic Cell, and Field Effect Hole Mobility. Macromolecules, 2005, 38, 2253-2260.	2.2	161
8	Boosting the Photocatalytic Hydrogen Evolution Activity for D–π–A Conjugated Microporous Polymers by Statistical Copolymerization. Advanced Materials, 2021, 33, e2008498.	11.1	143
9	Adenine Tautomers:  Relative Stabilities, Ionization Energies, and Mismatch with Cytosine. Journal of Physical Chemistry A, 2006, 110, 4012-4020.	1.1	115
10	Effect of Linking Pattern of Dibenzothiophene- <i>S</i> , <i>S</i> -dioxide-Containing Conjugated Microporous Polymers on the Photocatalytic Performance. Macromolecules, 2018, 51, 9502-9508.	2.2	113
11	A Comprehensive Review on Separation Methods and Techniques for Single-Walled Carbon Nanotubes. Materials, 2010, 3, 3818-3844.	1.3	91
12	Substituent effect of conjugated microporous polymers on the photocatalytic hydrogen evolution activity. Journal of Materials Chemistry A, 2020, 8, 2404-2411.	5.2	91
13	Differentiation of ferrocene D5d and D5h conformers using IR spectroscopy. Journal of Organometallic Chemistry, 2012, 713, 51-59.	0.8	90
14	Simultaneous Discrimination of Handedness and Diameter of Single-Walled Carbon Nanotubes (SWNTs) with Chiral Diporphyrin Nanotweezers Leading to Enrichment of a Single Enantiomer of (6,5)-SWNTs. Journal of the American Chemical Society, 2010, 132, 10876-10881.	6.6	88
15	Theoretical Investigation of Single and Double Transition Metals Anchored on Graphyne Monolayer for Nitrogen Reduction Reaction. Journal of Physical Chemistry C, 2020, 124, 15295-15301.	1.5	79
16	Control Synthesis of Tubular Hyper-Cross-Linked Polymers for Highly Porous Carbon Nanotubes. ACS Applied Materials & Interfaces, 2017, 9, 20779-20786.	4.0	77
17	Realizing high hydrogen evolution activity under visible light using narrow band gap organic photocatalysts. Chemical Science, 2021, 12, 1796-1802.	3.7	77
18	Differential attraction and repulsion of Staphylococcus aureus and Pseudomonas aeruginosa on molecularly smooth titanium films. Scientific Reports, 2011, 1, 165.	1.6	76

#	Article	IF	CITATIONS
19	Peryleneâ€Containing Conjugated Microporous Polymers for Photocatalytic Hydrogen Evolution. Macromolecular Chemistry and Physics, 2017, 218, 1700049.	1.1	71
20	Understanding glycine conformation through molecular orbitals. Journal of Chemical Physics, 2005, 123, 214307.	1.2	64
21	New Diagnostic of the Most Populated Conformer of Tetrahydrofuran in the Gas Phase. Journal of Physical Chemistry A, 2007, 111, 4927-4933.	1.1	64
22	Fine Tuning of Fluorene-Based Dye Structures for High-Efficiency <i>p</i> -Type Dye-Sensitized Solar Cells. ACS Applied Materials & Interfaces, 2014, 6, 10614-10622.	4.0	64
23	Plasma-Enhanced Synthesis of Bioactive Polymeric Coatings from Monoterpene Alcohols: A Combined Experimental and Theoretical Study. Biomacromolecules, 2010, 11, 2016-2026.	2.6	63
24	Silver nanoparticle–carbon nanotube hybrid films: Preparation and electrochemical sensing. Electrochimica Acta, 2012, 74, 111-116.	2.6	63
25	Double transition metal atoms anchored on Graphdiyne as promising catalyst for electrochemical nitrogen reduction reaction. Journal of Materials Science and Technology, 2021, 77, 244-251.	5.6	63
26	Assessment of Quantum Mechanical Models Based on Resolved Orbital Momentum Distributions of n-Butane in the Outer Valence Shell. Journal of Physical Chemistry A, 2003, 107, 10199-10207.	1.1	60
27	Experimental and Theoretical Electron Momentum Spectroscopic Study of the Valence Electronic Structure of Tetrahydrofuran under Pseudorotation. Journal of Physical Chemistry A, 2008, 112, 11078-11087.	1.1	56
28	The effect of molecular structure and fluorination on the properties of pyrene-benzothiadiazole-based conjugated polymers for visible-light-driven hydrogen evolution. Polymer Chemistry, 2018, 9, 4468-4475.	1.9	56
29	Graphene oxide nanoparticles for enhanced photothermal cancer cell therapy under the irradiation of a femtosecond laser beam. Journal of Biomedical Materials Research - Part A, 2014, 102, 2181-2188.	2.1	54
30	Conjugated random and alternating 2,3,4,5-tetraphenylsilole-containing polyfluorenes: Synthesis, characterization, strong solution photoluminescence, and light-emitting diodes. Polymer, 2005, 46, 8422-8429.	1.8	53
31	Modulated Charge Injection in p-Type Dye-Sensitized Solar Cells Using Fluorene-Based Light Absorbers. ACS Applied Materials & Interfaces, 2014, 6, 3448-3454.	4.0	48
32	Tetra-armed conjugated microporous polymers for gas adsorption and photocatalytic hydrogen evolution. Science China Chemistry, 2017, 60, 1075-1083.	4.2	46
33	Simultaneous Discrimination of Diameter, Handedness, and Metallicity of Single-Walled Carbon Nanotubes with Chiral Diporphyrin Nanocalipers. Journal of the American Chemical Society, 2013, 135, 4805-4814.	6.6	45
34	Norbornane: An investigation into its valence electronic structure using electron momentum spectroscopy, and density functional and Green's function theories. Journal of Chemical Physics, 2004, 121, 10525-10541.	1.2	43
35	ADENINE TAUTOMER ELECTRONIC STRUCTURAL SIGNATURES STUDIED USING DUAL SPACE ANALYSIS. Journal of Theoretical and Computational Chemistry, 2005, 04, 247-264.	1.8	43
36	Toward rational design of organic dye sensitized solar cells (DSSCs): An application to the TA-St-CA dye. Journal of Molecular Graphics and Modelling, 2013, 40, 64-71.	1.3	42

#	Article	IF	CITATIONS
37	Poly(dibenzothiophene-S,S-dioxide) with visible light-induced hydrogen evolution rate up to 44.2â€ <sup>-</sup> mmol hâ^'1 gâ^'1 promoted by K2HPO4. Applied Catalysis B: Environmental, 2020, 261, 118230.	10.8	40
38	Dibenzothiophene-S,S-dioxide-containing conjugated polymer with hydrogen evolution rate up to 147ÂmmolÂgâ ``1 hâ ``1. Applied Catalysis B: Environmental, 2022, 307, 121144.	10.8	40
39	Diameter-based separation of single-walled carbon nanotubes through selective extraction with dipyrene nanotweezers. Chemical Science, 2011, 2, 862.	3.7	39
40	Conjugated Microporous Polytetra(2â€Thienyl)ethylene as High Performance Anode Material for Lithium―and Sodiumâ€Ion Batteries. Macromolecular Chemistry and Physics, 2018, 219, 1700524.	1.1	39
41	Coexistence of 1,3-butadiene conformers in ionization energies and Dyson orbitals. Journal of Chemical Physics, 2005, 123, 124315.	1.2	38
42	Electronic Structure of the Azide Group in 3¢-Azido-3¢-deoxythymidine (AZT) Compared to Small Azide Compounds. Molecules, 2009, 14, 2656-2668.	1.7	37
43	Orbital Signatures of Methyl inl-Alanine. Journal of Physical Chemistry B, 2006, 110, 9713-9719.	1.2	36
44	Hypercrosslinked microporous organic polymer networks derived from silole-containing building blocks. Polymer, 2014, 55, 5746-5750.	1.8	36
45	Dominant Carbons in <i>trans</i> - and <i>cis</i> -Resveratrol Isomerization. Journal of Physical Chemistry B, 2017, 121, 4745-4755.	1.2	36
46	Hierarchical porous carbon activated by CaCO3 from pigskin collagen for CO2 and H2 adsorption. Microporous and Mesoporous Materials, 2018, 260, 172-179.	2.2	36
47	Microwave spectra of the Ne–N2 Van der Waals complex: Experiment and theory. Journal of Chemical Physics, 1998, 109, 5420-5432.	1.2	34
48	A Density Functional Theory and Electron Momentum Spectroscopy Study into the Complete Valence Electronic Structure of Cubane. Journal of the American Chemical Society, 2000, 122, 3892-3900.	6.6	34
49	A heptacyclic carbon–oxygen-bridged ladder-type building block for A–D–A acceptors. Materials Chemistry Frontiers, 2018, 2, 1716-1719.	3.2	34
50	Electronic Structure Study of the N2O Isomers Using Post-Hartreeâ^'Fock and Density Functional Theory Calculations. Journal of Physical Chemistry A, 2000, 104, 1304-1310.	1.1	33
51	Methylation of Zebularine: A Quantum Mechanical Study Incorporating Interactive 3D pdf Graphs. Journal of Physical Chemistry B, 2009, 113, 11496-11504.	1.2	33
52	Optical Resolution of Single-Walled Carbon Nanotubes through Molecular Recognition with Chiral Diporphyrin Nanotweezers. Chemistry Letters, 2010, 39, 1022-1027.	0.7	30
53	Dynamical (e,2e) studies of tetrahydrofurfuryl alcohol. Journal of Chemical Physics, 2012, 136, 244301.	1.2	30
54	Structure evolution of azo-fused conjugated microporous polymers for high performance lithium-ion batteries anodes. Journal of Power Sources, 2020, 453, 227868.	4.0	30

#	Article	IF	CITATIONS
55	Investigation into the Valence Electronic Structure of Norbornene Using Electron Momentum Spectroscopy, Green's Function, and Density Functional Theories. Journal of Physical Chemistry A, 2005, 109, 9324-9340.	1.1	28
56	Correlation of electronic structures of three cyclic dipeptides with their photoemission spectra. Journal of Chemical Physics, 2010, 133, 174319.	1.2	28
57	First-principle investigation of hydrogen solubility and diffusivity in transition metal-doped vanadium membranes and their mechanical properties. Journal of Alloys and Compounds, 2019, 805, 747-756.	2.8	28
58	Facile preparation of MnO/nitrogen-doped porous carbon nanotubes composites and their application in energy storage. Journal of Power Sources, 2019, 426, 33-39.	4.0	28
59	Improved selectivity in discriminating handedness and diameter of single-walled carbon nanotubes with N-substituted 3,6-carbazolylene-bridged chiral diporphyrin nanotweezers. Nanoscale, 2011, 3, 4117.	2.8	27
60	Photoelectron spectra and structures of three cyclic dipeptides: PhePhe, TyrPro, and HisGly. Journal of Chemical Physics, 2012, 136, 124301.	1.2	27
61	Stereochemical analysis of ferrocene and the uncertainty of fluorescence XAFS data. Journal of Synchrotron Radiation, 2012, 19, 145-158.	1.0	27
62	Discovery of new HER2/EGFR dual kinase inhibitors based on the anilinoquinazoline scaffold as potential anti-cancer agents. Journal of Enzyme Inhibition and Medicinal Chemistry, 2014, 29, 215-222.	2.5	27
63	Pyrene-alt-dibenzothiophene-S,S-dioxide copolymers for highly efficient photocatalytic hydrogen production: The role of linking pattern. Applied Surface Science, 2019, 495, 143537.	3.1	27
64	Orbital based electronic structural signatures of the guanine keto G-7H/G-9H tautomer pair as studied using dual space analysis. Biophysical Chemistry, 2006, 121, 105-120.	1.5	26
65	Inner-shell chemical shift of DNA/RNA bases and inheritance from their parent purine and pyrimidine. Journal of Synchrotron Radiation, 2008, 15, 624-631.	1.0	26
66	Valence orbital response to pseudorotation of tetrahydrofuran: A snapshot using dual space analysis. Journal of Chemical Physics, 2008, 128, 125102.	1.2	26
67	In silico design: Extended molecular dynamic simulations of a new series of dually acting inhibitors against EGFR and HER2. Journal of Molecular Graphics and Modelling, 2013, 44, 220-231.	1.3	26
68	Theoretical investigation of molybdenum/tungsten-vanadium solid solution alloy membranes: Thermodynamic stability and hydrogen permeation. Journal of Membrane Science, 2020, 608, 118200.	4.1	26
69	The attachment of amino fragment to purine: inner-shell structures and spectra. Journal of Synchrotron Radiation, 2008, 15, 151-157.	1.0	25
70	Optical Resolution and Diameter-Based Enrichment of Single-Walled Carbon Nanotubes through Simultaneous Recognition of Their Helicity and Diameter with Chiral Monoporphyrin. Journal of Physical Chemistry C, 2009, 113, 9108-9113.	1.5	25
71	Intramolecular interactions of L-phenylalanine revealed by inner shell chemical shift. Journal of Chemical Physics, 2009, 131, 044321.	1.2	24
72	A high performance and low cost poly(dibenzothiophene- <i>S</i> , <i>S</i> -dioxide)@TiO <sub>2</sub> composite with hydrogen evolution rate up to 51.5 mmol h <sup>â^`1</sup> g <sup>â^`1</sup> . Journal of Materials Chemistry A, 2020, 8, 18292-18301.	5.2	23

#	Article	IF	CITATIONS
73	Valence bond and molecular orbital studies of three N2O isomers, and valence bond representations for some azide decompositions. Journal of Molecular Modeling, 2001, 7, 271-277.	0.8	22
74	Preferential extraction of left- or right-handed single-walled carbon nanotubes by use of chiral diporphyrin nanotweezers. Organic and Biomolecular Chemistry, 2012, 10, 5830.	1.5	22
75	Targeting the Achilles heel of the hepatitis B virus: a review of current treatments against covalently closed circular DNA. Drug Discovery Today, 2015, 20, 548-561.	3.2	22
76	Ab initio rotationally resolved infrared spectrum of potassium-lithium (K2Li+). The Journal of Physical Chemistry, 1992, 96, 6158-6165.	2.9	21
77	Inner valence shell bonding mechanism of n-butane studied using orbital momentum distributions of its conformational isomers. Journal of Physics B: Atomic, Molecular and Optical Physics, 2004, 37, 557-569.	0.6	21
78	Effect of positron–atom interactions on the annihilation gamma spectra of molecules. New Journal of Physics, 2012, 14, 035021.	1.2	21
79	A study of aliphatic amino acids using simulated vibrational circular dichroism and Raman optical activity spectra. European Physical Journal D, 2013, 67, 1.	0.6	21
80	A novel off-on fluorescent chemosensor for Al <sup>3+</sup> derived from a 4,5-diazafluorene Schiff base derivative. RSC Advances, 2018, 8, 31889-31894.	1.7	21
81	Switching on optical properties of D-ï€-A DSSC sensitizers from ï€-spacers towards machine learning. Solar Energy, 2019, 188, 1189-1200.	2.9	21
82	Accurate X-ray Absorption Spectra of Dilute Systems: Absolute Measurements and Structural Analysis of Ferrocene and Decamethylferrocene. Journal of Physical Chemistry C, 2016, 120, 9399-9418.	1.5	20
83	Building an electron push–pull system of linear conjugated polymers for improving photocatalytic hydrogen evolution efficiency. Polymer Bulletin, 2019, 76, 3195-3206.	1.7	20
84	Bisulfoneâ€Functionalized Organic Polymer Photocatalysts for Highâ€Performance Hydrogen Evolution. ChemSusChem, 2020, 13, 369-375.	3.6	20
85	The electronic structural information from core orbitals of norbornadiene, norbornene and norbornane. Computational and Theoretical Chemistry, 2005, 728, 31-42.	1.5	19
86	Intramolecular interactions of <scp>L</scp> â€phenylalanine: Valence ionization spectra and orbital momentum distributions of its fragment molecules. Journal of Computational Chemistry, 2011, 32, 525-535.	1.5	19
87	Photoelectron Spectra and Electronic Structures of the Radiosensitizer Nimorazole and Related Compounds. Journal of Physical Chemistry A, 2015, 119, 9986-9995.	1.1	19
88	A Turn-on and Reversible Fluorescence Sensor for Zinc Ion Based on 4,5-Diazafluorene Schiff Base. Journal of Fluorescence, 2016, 26, 1555-1561.	1.3	19
89	An electron momentum spectroscopy and density functional theory study of the outer valence electronic structure of stella-2,6-dione. Journal of Physics B: Atomic, Molecular and Optical Physics, 2003, 36, 3155-3171.	0.6	18
90	Adsorption of Cytosine and AZA Derivatives of Cytidine on Au Single Crystal Surfaces. Journal of Physical Chemistry C, 2013, 117, 18423-18433.	1.5	18

#	Article	IF	CITATIONS
91	Assessment of new anti-HER2 ligands using combined docking, QM/MM scoring and MD simulation. Journal of Molecular Graphics and Modelling, 2013, 40, 91-98.	1.3	18
92	Discovery of Novel Peptidomimetics as Irreversible <scp>CHIKV</scp> Ns <scp>P</scp> 2 Protease Inhibitors Using Quantum Mechanicalâ€Based Ligand Descriptors. Chemical Biology and Drug Design, 2015, 86, 1518-1527.	1.5	18
93	Low-bandgap conjugated polymers based on alkylthiothienyl-substituted benzodithiophene for efficient bulk heterojunction polymer solar cells. Polymer, 2017, 122, 96-104.	1.8	18
94	Thiophene-rich conjugated microporous polymers as anode materials for high performance lithium- and sodium-ion batteries. Solid State Ionics, 2020, 347, 115247.	1.3	18
95	Dipole moment surfaces and the mid- and far-IR spectra of N2-Ar. Journal of Chemical Physics, 2000, 113, 98-106.	1.2	17
96	Comprehensive Experimental and Theoretical Study into the Complete Valence Electronic Structure of Norbornadiene. Journal of Physical Chemistry A, 2002, 106, 9573-9581.	1.1	17
97	Definitive confirmation for through-space bond dominance in the outermost π-orbitals of norbornadiene. Journal of Electron Spectroscopy and Related Phenomena, 2002, 123, 389-395.	0.8	17
98	Blue shifted intramolecular Câ^'H···O improper hydrogen bonds in conformers of zidovudine. Chemical Physics Letters, 2010, 493, 358-363.	1.2	17
99	Positron scattering from chiral enantiomers. Physical Review A, 2012, 85, .	1.0	17
100	Gamma-ray spectra of hexane (C6H14) in positron–electron annihilation process. Radiation Physics and Chemistry, 2013, 89, 14-19.	1.4	17
101	First-principles study of Carbz-PAHTDDT dye sensitizer and two Carbz-derived dyes for dye sensitized solar cells. Journal of Molecular Modeling, 2014, 20, 2177.	0.8	17
102	Shifting UV-vis absorption spectrum through rational structural modifications of zinc porphyrin photoactive compounds. RSC Advances, 2016, 6, 15345-15353.	1.7	17
103	Mechanistic Insights into Direct Methane Oxidation to Methanol on Single-Atom Transition-Metal-Modified Graphyne. ACS Applied Nano Materials, 2021, 4, 12006-12016.	2.4	17
104	Exploring the electronic structure of 2,6-stelladione from momentum space I: the p-dominant molecular orbitals in the outer valence shell. Chemical Physics Letters, 2003, 382, 217-225.	1.2	16
105	Interfacial stress transfer of fiber pullout for carbon nanotubes with a composite coating. Journal of Materials Science, 2007, 42, 4191-4196.	1.7	16
106	Gamma-ray spectra of methane in the positron–electron annihilationprocess. Radiation Physics and Chemistry, 2013, 85, 59-63.	1.4	16
107	The d-electrons of Fe in ferrocene: the excess orbital energy spectrum (EOES). RSC Advances, 2015, 5, 11933-11941.	1.7	16
108	Two conformers of a tyrosine kinase inhibitor (AC-1478) disclosed using simulated UV-Vis absorption spectroscopy. New Journal of Chemistry, 2016, 40, 8296-8304.	1.4	16

#	Article	IF	CITATIONS
109	Enhanced photocatalytic activity of g-C3N4/MnO composites for hydrogen evolution under visible light. Dalton Transactions, 2019, 48, 14864-14872.	1.6	16
110	Variational calculation of the ro-vibrational states of Na3+. Molecular Physics, 1992, 77, 1197-1207.	0.8	15
111	Prediction of spectroscopic constants for diatomic molecules in the ground and excited states using time-dependent density functional theory. Journal of Computational Chemistry, 2006, 27, 163-173.	1.5	15
112	Throughput based temporal verification for monitoring large batch of parallel processes. , 2014, , .		15
113	Microporous organic polymers based on tetraethynyl building blocks with N-functionalized pore surfaces: synthesis, porosity and carbon dioxide sorption. RSC Advances, 2016, 6, 113826-113833.	1.7	15
114	Synthesis and photovoltaic properties of donor–acceptor conjugated polymers based on 4,7-dithienyl-2,1,3-benzothiadiazole functionalized silole. Synthetic Metals, 2016, 220, 433-439.	2.1	15
115	Element-free Galerkin scaled boundary method based on moving Kriging interpolation for steady heat conduction analysis. Engineering Analysis With Boundary Elements, 2019, 106, 440-451.	2.0	15
116	Variational calculations of rotationally resolved infrared properties of Li2Na+, LiNa2+ and KLiNa+. Journal of Molecular Structure, 1992, 272, 73-93.	1.8	14
117	Potential energy surface for and pure rotational spectra of isotopomeric Cl2–Ar van der Waals complexes. Journal of Chemical Physics, 1996, 104, 9304-9312.	1.2	14
118	Core molecular orbital contribution to N2O isomerization as studied using theoretical electron momentum spectroscopy. Spectrochimica Acta - Part A: Molecular and Biomolecular Spectroscopy, 2001, 57, 9-15.	2.0	14
119	A high-resolution electron momentum spectroscopy and density functional theory study into the complete valence electronic structure of allene. Journal of Computational Chemistry, 2001, 22, 1321-1333.	1.5	14
120	Molecular orbitals of methane: symmetry or hybridization?. Computational and Theoretical Chemistry, 2004, 678, 105-111.	1.5	14
121	Valence space electron momentum spectroscopy of diborane. Journal of Electron Spectroscopy and Related Phenomena, 2006, 151, 215-223.	0.8	14
122	Solvent effects on blue shifted improper hydrogen bond of C–Hâ⊄O in deoxycytidine isomers. Chemical Physics Letters, 2010, 500, 327-333.	1.2	14
123	Electron shell contributions to gamma-ray spectra of positron annihilation in noble gases. Journal of Physics B: Atomic, Molecular and Optical Physics, 2010, 43, 165207.	0.6	14
124	Photoelectron Spectra of Some Antibiotic Building Blocks: 2-Azetidinone and Thiazolidine-Carboxylic Acid. Journal of Physical Chemistry A, 2012, 116, 8653-8660.	1.1	14
125	Chemical structural effects on Î <sup>3</sup> -ray spectra of positron annihilation in fluorobenzenes. European Physical Journal D, 2012, 66, 1.	0.6	14
126	Effects of quantum chemistry models for bound electrons on positron annihilation spectra for atoms and small molecules. New Journal of Physics, 2012, 14, 085022.	1.2	14

#	Article	IF	CITATIONS
127	UV–Vis spectroscopy and solvatochromism of the tyrosine kinase inhibitor AG-1478. Spectrochimica Acta - Part A: Molecular and Biomolecular Spectroscopy, 2016, 164, 128-132.	2.0	14
128	Investigation of adsorption, dissociation, and diffusion properties of hydrogen on the V (1 0 0) surface and in the bulk: A first-principles calculation. Journal of Advanced Research, 2020, 21, 25-34.	4.4	14
129	The importance of the molecular weight of PEDOT hole transporting materials for efficient organic solar cells. Journal of Materials Chemistry C, 2020, 8, 17185-17193.	2.7	14
130	A Case Study on a Soluble Dibenzothiophene- <i>S</i> , <i>S</i> -dioxide-Based Conjugated Polyelectrolyte for Photocatalytic Hydrogen Production: The Film versus the Bulk Material. ACS Applied Materials & Interfaces, 2021, 13, 42753-42762.	4.0	14
131	Use of simulated infrared spectra to test N2-Ar pair potentials and dipole moment surfaces. Molecular Physics, 1996, 88, 821-840.	0.8	14
132	Chemical bonding mechanisms of n-butane probed by the core orbitals of conformational isomers in r-space and k-space. Chemical Physics Letters, 2004, 384, 144-149.	1.2	13
133	Impact of ketone and amino on the inner shell ofÂguanine. Journal of Synchrotron Radiation, 2009, 16, 545-552.	1.0	13
134	Density Functional Study on Core Ionization Spectra of Cytidine and Its Fragments. Bulletin of the Chemical Society of Japan, 2009, 82, 187-195.	2.0	13
135	In Silico Investigation of Lactone and Thiolactone Inhibitors in Bacterial Quorum Sensing Using Molecular Modeling. International Journal of Chemistry, 2013, 5, .	0.3	13
136	Ferrocene Orientation Determined Intramolecular Interactions Using Energy Decomposition Analysis. Materials, 2015, 8, 7723-7737.	1.3	13
137	Conformation Analysis of Ferrocene and Decamethylferrocene via Full-Potential Modeling of XANES and XAFS Spectra. Journal of Physical Chemistry Letters, 2016, 7, 2792-2796.	2.1	13
138	Reinterpretation of Dynamic Vibrational Spectroscopy to Determine the Molecular Structure and Dynamics of Ferrocene. Chemistry - A European Journal, 2016, 22, 18019-18026.	1.7	13
139	Electronic structure and intramolecular interactions in three methoxyphenol isomers. Journal of Chemical Physics, 2018, 149, 134312.	1.2	13
140	Insights into the dissociative ionization of glycine by PEPICO experiments. Physical Chemistry Chemical Physics, 2018, 20, 22841-22848.	1.3	13
141	The electronic structure of small lithium clusters. Journal of Cluster Science, 1991, 2, 203-217.	1.7	12
142	Ab initio calculations of the rotationally resolved infrared spectrum of KNa 2 +. Theoretica Chimica Acta, 1994, 88, 131-145.	0.9	12
143	An electron momentum spectroscopy and density functional theory investigation into the complete valence electronic structure of ethylene oxide. Journal of Physics B: Atomic, Molecular and Optical Physics, 1999, 32, 3239-3253.	0.6	12
144	An (e,2e) coincidence study of formic acid monomer and dimer. Chemical Physics Letters, 2008, 451, 18-24.	1.2	12

#	Article	IF	CITATIONS
145	Differentiation of alkane isomers through binding energy spectra and total momentum cross sections. New Journal of Chemistry, 2014, 38, 1031.	1.4	12
146	Molecular dynamics studies on the NMR structures of rabbit prion protein wild type and mutants: surface electrostatic charge distributions. Journal of Biomolecular Structure and Dynamics, 2015, 33, 1326-1335.	2.0	12
147	Novel 4,5-diazafluorene-based Schiff base derivatives as Al 3+ ions fluorescence turn-on sensors. Synthetic Metals, 2016, 217, 37-42.	2.1	12
148	Hypercrosslinked silole ontaining microporous organic polymers with <scp>N</scp> â€functionalized pore surfaces for gas storage and separation. Journal of Applied Polymer Science, 2018, 135, 45907.	1.3	12
149	Differentiation of adenine non-planarity in valence molecular orbitals. Molecular Simulation, 2006, 32, 667-673.	0.9	11
150	Docking Positrophilic Electrons into Molecular Attractive Potentials of Fluorinated Methanes. Journal of the Physical Society of Japan, 2013, 82, 104301.	0.7	11
151	Synthesis of π-Extended Dithienobenzodithiophene-Containing Medium Bandgap Copolymers and Their Photovoltaic Application. Journal of Macromolecular Science - Pure and Applied Chemistry, 2015, 52, 934-941.	1.2	11
152	Synthesis and Photovoltaic Properties of 2D-Conjugated Polymers Based on Alkylthiothienyl-Substituted Benzodithiophene and Different Accepting Units. Polymers, 2018, 10, 331.	2.0	11
153	Valence Orbital Electron Momentum Spectroscopy For N2O. Journal of Physical Chemistry A, 2001, 105, 1254-1259.	1.1	10
154	Intramolecular proton transfer in adenine imino tautomers. Molecular Simulation, 2006, 32, 1261-1270.	0.9	10
155	Effects of alkyl side chains on properties of aliphatic amino acids probed using quantum chemical calculations. Journal of Synchrotron Radiation, 2011, 18, 733-742.	1.0	10
156	Density functional study of Cu2+-phenylalanine complex under micro-solvation environment. Journal of Molecular Graphics and Modelling, 2013, 45, 180-191.	1.3	10
157	Rational use of ligand to shift the UV–vis spectrum of Ru-complex sensitiser dyes for DSSC applications. Radiation Physics and Chemistry, 2019, 161, 66-71.	1.4	10
158	Radiation Damage Mechanisms of Chemotherapeutically Active Nitroimidazole Derived Compounds. Frontiers in Chemistry, 2019, 7, 329.	1.8	10
159	Variational calculations of rovibrational states of Li2K+. Chemical Physics, 1993, 172, 247-258.	0.9	9
160	A Closed-loop Transcutaneous Power Transmission System with Thermal Control for Artificial Urethral Valve Driven by SMA Actuator. Journal of Intelligent Material Systems and Structures, 2006, 17, 779-786.	1.4	9
161	Enrichment of Large-Diameter Single-Walled Carbon Nanotubes (SWNTs) with Metallo-Octaethylporphyrins. Materials, 2013, 6, 3064-3078.	1.3	9
162	From building blocks of proteins to drugs: a quantum chemical study on structure–property relationships of phenylalanine, tyrosine and dopa. RSC Advances, 2014, 4, 8617.	1.7	9

#	Article	IF	CITATIONS
163	Enhanced solubilization of large-diameter single-walled carbon nanotubes with amino-functionalized dipyrene nanotweezers. Journal of Materials Science, 2015, 50, 6032-6040.	1.7	9
164	A theoretical study of core excitation spectra of NO molecule. Journal of Physics B: Atomic, Molecular and Optical Physics, 1998, 31, 1649-1656.	0.6	8
165	Structural impact on the methano bridge in norbornadiene, norbornene and norbornane. Journal of Physics and Chemistry of Solids, 2004, 65, 2041-2054.	1.9	8
166	lonisation energy splitting of amino and imino N–K sites in cytidine. Micro and Nano Letters, 2006, 1, 23.	0.6	8
167	Applications of ionization spectroscopy to study small bio-molecules. Journal of Physics: Conference Series, 2008, 141, 012019.	0.3	8
168	Calculation of Gamma Spectra for Positron Annihilation on Molecules. Materials Science Forum, 2010, 666, 21-24.	0.3	8
169	Calculations of gamma-ray spectral profiles of linear alkanes in the positron annihilation process. Journal of Electron Spectroscopy and Related Phenomena, 2014, 196, 146-151.	0.8	8
170	Structures of Cycloserine and 2-Oxazolidinone Probed by X-ray Photoelectron Spectroscopy: Theory and Experiment. Journal of Physical Chemistry A, 2014, 118, 3645-3654.	1.1	8
171	Synthesis and characterization of alternating and random conjugated polymers derived from dithieno[2,3-d:2′,3′-d′]benzo[1,2-b:4,5-b′]dithiophene and 2,1,3-benzothiadiazole derivatives. Polymer Journal, 2015, 47, 803-809.	r <b>1</b> .3	8
172	Synthesis and Characterization of Functional Triphenylphosphine ontaining Microporous Organic Polymers for Gas Storage and Separation. Macromolecular Chemistry and Physics, 2017, 218, 1700275.	1.1	8
173	Electron Momentum Spectroscopy and Its Applications to Molecules of Biological Interest. AIP Conference Proceedings, 2007, , .	0.3	7
174	Valence orbital response to conformers ofn-butane. Molecular Simulation, 2007, 33, 1173-1185.	0.9	7
175	Unsaturated Didehydrodeoxycytidine Drugs. 1. Impact of CC Positions in the Sugar Ring. Journal of Physical Chemistry B, 2007, 111, 9628-9633.	1.2	7
176	Theoretical investigation of the electron capture and loss processes in the collisions of He2+ + Ne. Journal of Chemical Physics, 2013, 139, 084321.	1.2	7
177	Molecular dynamics studies on the buffalo prion protein. Journal of Biomolecular Structure and Dynamics, 2016, 34, 762-777.	2.0	7
178	Conformational Plasticity in Tyrosine Kinase Inhibitor–Kinase Interactions Revealed with Fluorescence Spectroscopy and Theoretical Calculations. Journal of Physical Chemistry B, 2018, 122, 4667-4679.	1.2	7
179	Synergetic Effect of Perfluorooctanoic Acid on the Preparation of Poly(3,4â€ethylenedioxythiophene): Lignosulfonate Aqueous Dispersions with High Film Conductivity. ChemistrySelect, 2019, 4, 11406-11412.	0.7	7
180	Ab Initio Ro-Vibrational Structure of the C2? Isotopes of H2O+. Australian Journal of Physics, 1992, 45, 651.	0.6	7

#	Article	IF	CITATIONS
181	An Eckart–Watson Hamiltonian for linear molecules in the rectilinear displacement w -coordinates and an application to HCN. Computational and Theoretical Chemistry, 2000, 497, 227-240.	1.5	6
182	Direct observations of the chemical shift and electron momentum distributions of core shell in N2O. Chemical Physics Letters, 2006, 422, 308-312.	1.2	6
183	An experimental and theoretical study into the valence electronic structure of bicyclo[2.2.1]hepta-2,5-dione. Journal of Physics B: Atomic, Molecular and Optical Physics, 2006, 39, 2411-2429.	0.6	6
184	Effects of diode current on high power microwave generation in a vircator. Journal of Plasma Physics, 2009, 75, 787-798.	0.7	6
185	Hydroxyapatite Whisker Effect on Strength of Calcium Phosphate Bone Cement. Advanced Materials Research, 0, 534, 30-33.	0.3	6
186	X-ray Photoemission Spectra and Electronic Structure of Coumarin and its Derivatives. Journal of Physical Chemistry A, 2016, 120, 7080-7087.	1.1	6
187	A review on the salt bridge ASP177-ARG163 (O–N) of wild-type rabbit prion protein. Journal of Biomolecular Structure and Dynamics, 2016, 34, 1020-1028.	2.0	6
188	Quantum chemical approach for positron annihilation spectra of atoms and molecules beyond plane-wave approximation. Journal of Chemical Physics, 2018, 148, 184110.	1.2	6
189	Impact of intramolecular hydrogen bonding of gallic acid conformers on chemical shift through NMR spectroscopy. Journal of Molecular Graphics and Modelling, 2020, 95, 107486.	1.3	6
190	Experimental and Theoretical Soft X-ray Study of Nicotine and Related Compounds. Journal of Physical Chemistry A, 2020, 124, 4025-4035.	1.1	6
191	Red-Edge Excitation Shift Spectroscopy (REES): Application to Hidden Bound States of Ligands in Protein–Ligand Complexes. International Journal of Molecular Sciences, 2021, 22, 2582.	1.8	6
192	Accelerating optical reporting for conformation of tyrosine kinase inhibitors in solutions. International Journal of Quantum Chemistry, 2021, 121, e26765.	1.0	6
193	Positional and Conformational Isomerism in Hydroxybenzoic Acid: A Core-Level Study and Comparison with Phenol and Benzoic Acid. Journal of Physical Chemistry A, 2021, 125, 9877-9891.	1.1	6
194	SVD Analysis in Fitting Property Surfaces. Journal of the Chinese Chemical Society, 1992, 39, 339-341.	0.8	5
195	Ab initio rovibrational states of the D3h and C2v isotopomers of Li3+. Spectrochimica Acta - Part A: Molecular and Biomolecular Spectroscopy, 1995, 51, 1827-1835.	2.0	5
196	Influence of ground-state geometry on carbon monoxide x-ray emission spectral profiles. Journal of Physics B: Atomic, Molecular and Optical Physics, 1998, 31, 3513-3525.	0.6	5
197	A quantum mechanical study of bioactive 3-chloro-2,5-dihydroxybenzyl alcohol through substitutions. Theoretical Chemistry Accounts, 2011, 130, 965-979.	0.5	5
198	Electronic structures of hexane isomers studied using quantum mechanics and graph theory. Journal of Theoretical and Computational Chemistry, 2015, 14, 1550014.	1.8	5

#	Article	IF	CITATIONS
199	How different is pyrimidine as a core component of DNA base from its diazine isomers: A DFT study?. International Journal of Quantum Chemistry, 2016, 116, 1836-1845.	1.0	5
200	How similar is the electronic structures of $\hat{I}^2$ -lactam and alanine?. Radiation Physics and Chemistry, 2016, 119, 1-8.	1.4	5
201	Micro-solvation of tyrosine-kinase inhibitor AG1478 explored with fluorescence spectroscopy and computational chemistry. RSC Advances, 2017, 7, 31725-31735.	1.7	5
202	Effects of Mo alloying on stability and diffusion of hydrogen in the Nb16H phase: a first-principles investigation. RSC Advances, 2019, 9, 19495-19500.	1.7	5
203	Methodologies in Spectral Tuning of DSSC Chromophores through Rational Design and Chemical-Structure Engineering. Materials, 2019, 12, 4024.	1.3	5
204	Resolution of ferrocene and deuterated ferrocene conformations using dynamic vibrational spectroscopy: Experiment and theory. Inorganica Chimica Acta, 2020, 506, 119491.	1.2	5
205	Synthesis and characterisation of monolithic <scp>PTFE</scp> â€modified <scp>MnO<sub>X</sub></scp> / <scp>FeO<sub>X</sub></scp> catalysts for selective catalytic reduction ( <scp>SCR</scp> ) of <scp>NO<sub>X</sub></scp> at low temperature. Journal of Chemical Technology and Biotechnology, 2021, 96, 1016-1029.	1.6	5
206	Eliminating the Detrimental Effect of Secondary Doping on PEDOT : PSS Hole Transporting Material Performance. ChemSusChem, 2021, 14, 4802-4811.	3.6	5
207	A THEORETICAL STUDY ON DUAL FLUORESCENCE OF 4-DIMETHYLAMINOPYRIDINE BY POLARIZABLE CONTINUUM MODEL. Journal of Theoretical and Computational Chemistry, 2008, 07, 821-832.	1.8	4
208	Influence of functional groups on the Cα–Cβ chain of I-phenylalanine and its derivatives. Nuclear Instruments and Methods in Physics Research, Section A: Accelerators, Spectrometers, Detectors and Associated Equipment, 2010, 619, 143-146.	0.7	4
209	Performance assessment of density functional theory-based models using orbital momentum distributions. Molecular Simulation, 2012, 38, 468-480.	0.9	4
210	A New Particle Swarm Optimization-Based Strategy for Cost-Effective Data Placement in Scientific Cloud Workflows. Lecture Notes in Electrical Engineering, 2014, , 115-120.	0.3	4
211	Fragment based electronic structural analysis of <scp>l</scp> -phenylalanine using calculated ionization spectroscopy and dual space analysis. RSC Advances, 2014, 4, 60597-60608.	1.7	4
212	Sitting above the maze: recent model discoveries in molecular science. Molecular Simulation, 2015, 41, 205-229.	0.9	4
213	Exploring the optical reporting characteristics of drugs: UV-Vis spectra and conformations of the tyrosine kinase inhibitor SKF86002. New Journal of Chemistry, 2017, 41, 14567-14573.	1.4	4
214	Solvatochromism and linear solvation energy relationship of the kinase inhibitor SKF86002. Spectrochimica Acta - Part A: Molecular and Biomolecular Spectroscopy, 2017, 170, 226-233.	2.0	4
215	Significant improved selectivity of a fluorescent sensor for Al3+ made from a fluorinated rhodamine B Schiff base. Research on Chemical Intermediates, 2019, 45, 1815-1827.	1.3	4
216	Deducing the Conformational Properties of a Tyrosine Kinase Inhibitor in Solution by Optical Spectroscopy and Computational Chemistry. Frontiers in Chemistry, 2020, 8, 596.	1.8	4

#	Article	IF	CITATIONS
217	Molecular dynamics study of ferrocene topology under various temperatures. International Journal of Quantum Chemistry, 2020, 120, e26398.	1.0	4
218	Robust design of D-ï€-A model compounds using digital structures for organic DSSC applications. Journal of Molecular Graphics and Modelling, 2021, 102, 107798.	1.3	4
219	Solvent contribution to ferrocene conformation: Theory and experiment. Radiation Physics and Chemistry, 2021, 189, 109697.	1.4	4
220	Switching On/Off the Intramolecular Hydrogen Bonding of 2-Methoxyphenol Conformers: An NMR Study. Australian Journal of Chemistry, 2020, 73, 222.	0.5	4
221	Synthesis and Gas Sorption Properties of Microporous Poly(arylene ethynylene) Frameworks. Acta Chimica Sinica, 2017, 75, 473.	0.5	4
222	The electronic structure of small sodium clusters. Journal of Cluster Science, 1992, 3, 229-246.	1.7	3
223	Ab initio and analytical potential energy functions of K2Na+. Journal of Molecular Structure, 1996, 376, 449-459.	1.8	3
224	Ab initio potential energy surface and vibrational energies of Li3â^'. Chemical Physics Letters, 1997, 269, 138-144.	1.2	3
225	Separation of Left- and Right-Handed Structures of Single-Walled Carbon Nanotubes through Molecular Recognition. World Scientific Series on Carbon Nanoscience, 2012, , 203-232.	0.1	3
226	Valence structures of aromatic bioactive compounds: a combined theoretical and experimental study. Journal of Synchrotron Radiation, 2012, 19, 773-781.	1.0	3
227	A facile approach to synthesize SiO2 · Re2O3 (Re = Y, Eu, La, Sm, Tb, Pr) hollow sphere and it in drug release. Nanoscale Research Letters, 2013, 8, 435.	ts applicat	ion <sub>3</sub>
228	Study of Nano-Hydroxyapatite Adsorption in Heavy Metals. Advanced Materials Research, 2013, 777, 15-18.	0.3	3
229	Logistics scheduling based on cloud business workflows. , 2014, , .		3
230	Theoretical study of valence orbital response to guanine tautomerization in coordinate and momentum spaces. Journal of Physics B: Atomic, Molecular and Optical Physics, 2015, 48, 205101.	0.6	3
231	Combined SRCT & FXCT $\hat{a} \in $ The next steps. Journal of Instrumentation, 2016, 11, C03048-C03048.	0.5	3
232	A pH-induced conformational switch in a tyrosine kinase inhibitor identified by electronic spectroscopy and quantum chemical calculations. Scientific Reports, 2017, 7, 16271.	1.6	3
233	Resveratrol's Hidden Hand: A Route to the Optical Detection of Biomolecular Binding. Journal of Physical Chemistry B, 2018, 122, 2841-2850.	1.2	3
234	Reduced order model analysis method via proper orthogonal decomposition for nonlinear transient heat conductionproblems. Scientia Sinica: Physica, Mechanica Et Astronomica, 2018, 48, 124603.	0.2	3

#	Article	IF	CITATIONS
235	Theoretical study of excitation and radiative de-excitation characteristics for the NO molecule. Journal of Physics B: Atomic, Molecular and Optical Physics, 1998, 31, 3789-3802.	0.6	2
236	The invariant character of two-body binding potentials. Computational and Theoretical Chemistry, 2003, 664-665, 83-89.	1.5	2
237	Outer valence orbital response to proton positions in prototropic tautomers of adenine. Journal of Computational Methods in Sciences and Engineering, 2007, 6, 251-267.	0.1	2
238	N-K spectra of adenine amino tautomers. Journal of Physics: Conference Series, 2009, 185, 012040.	0.3	2
239	Methylation of zebularine investigated using density functional theory calculations. Journal of Computational Chemistry, 2011, 32, 2077-2083.	1.5	2
240	Damage Evaluation of Supercritical CO <sub>2</sub> for Hydronibrile Nitrile(HNBR). Advanced Materials Research, 2012, 476-478, 2582-2585.	0.3	2
241	The impact of candidate display styles for Japanese and Chinese characters on input efficiency. International Journal of Human Computer Studies, 2013, 71, 236-249.	3.7	2
242	NMR Chemical Shift and Methylation of 4-Nitroimidazole: Experiment and Theory. Australian Journal of Chemistry, 2021, 74, 48.	0.5	2
243	Dominance of eclipsed ferrocene conformer in solutions revealed by the IR spectra between 400 and 500 cm-1. Radiation Physics and Chemistry, 2021, 188, 109590.	1.4	2
244	Health Identification of Water Resources-Ecological-Socioeconomic System of Baiyangdian Wetland. Advanced Materials Research, 0, 183-185, 2340-2345.	0.3	1
245	Geometrically Nonlinear Analysis of Composite Girder Cable-Stayed Bridge with Three Towers in Completion Stage. Applied Mechanics and Materials, 2012, 166-169, 2761-2764.	0.2	1
246	Impact of Electric Vehicle Charging Mode on Load Characteristic in the Shandong Electric Power Grid. Advanced Materials Research, 2012, 608-609, 1582-1586.	0.3	1
247	Performance assessment of density functional methods with Gaussian and Slater basis sets using $7 lf$ orbital momentum distributions of N[sub 2]O. , 2012, , .		1
248	Design of Greenhouse Monitoring System Based on Zigbee. Advanced Materials Research, 0, 655-657, 773-776.	0.3	1
249	Inheritance and correlation of nucleic acid pyrimidine bases. International Journal of Quantum Chemistry, 2013, , n/a-n/a.	1.0	1
250	A Survey and a Molecular Dynamics Study on the (Central) Hydrophobic Region of Prion Proteins. Current Pharmaceutical Biotechnology, 2014, 15, 1026-1048.	0.9	1
251	An experimental and theoretical investigation of XPS and NEXAFS of nicotine, nicotinamide, and nicotinc acid. Journal of Physics: Conference Series, 2020, 1412, 102008.	0.3	1
252	Theoretical and Experimental Models of Molecules Illustrated with Quantum-Chemical Calculations of Electronic Structure of H2CN2 Isomers. , 2008, , 341-364.		1

#	Article	IF	CITATIONS
253	Differentiation of alkyl radicals: A route through chemical graph theory. International Journal of Quantum Chemistry, 2021, 121, e26567.	1.0	1
254	Probing Intramolecular Interaction of Stereoisomers Using Computational Spectroscopy. Australian Journal of Chemistry, 2020, 73, 813.	0.5	1
255	Optical spectra and conformation pool of tyrosine kinase inhibitor PD153035 using a robust quantum mechanical conformation search. New Journal of Chemistry, 0, , .	1.4	1
256	Variational calculations for the rovibrational states of Si212C and Si213C. Spectrochimica Acta - Part A: Molecular and Biomolecular Spectroscopy, 1996, 52, 1581-1592.	2.0	0
257	Variational calculations of the rovibrational energy levels of K2Na+. Chemical Physics Letters, 1996, 261, 51-56.	1.2	0
258	A Study on the F-T Characteristics of Thickness Modes of Doubly Rotated Y-cut Piezoelectric Quartz Crystal. Journal of Intelligent Material Systems and Structures, 2006, 17, 695-699.	1.4	0
259	Cracking Analysis of Q235-B Steel Plate in Cold-Bend Process. Advanced Materials Research, 0, 156-157, 1586-1589.	0.3	0
260	Temperature Controlling and Monitoring of Mass Concrete Construction of Suspension Bridge Anchorage. Applied Mechanics and Materials, 2011, 71-78, 1911-1914.	0.2	0
261	Study on Space Nonlinear FE Model of Composite Beam Cable-Stayed Bridge with Three Towers. Applied Mechanics and Materials, 0, 90-93, 975-978.	0.2	0
262	A Finite Element Analysis of the Normal Combination Round and Spline Broach Based on ANSYS. Advanced Materials Research, 0, 383-390, 1831-1836.	0.3	0
263	A Finite Element Analysis of the Normal Combination Round and Spline Broach Based on ANASYS. Advanced Materials Research, 0, 433-440, 6551-6557.	0.3	0
264	Study and Practice on the Whole Process Evaluation Strategies of Green Building. Advanced Materials Research, 2012, 608-609, 1686-1689.	0.3	0
265	Temperature Sensitivity Analysis of Massive Concrete Mixing with Slag Powder and Fly Ash. Advanced Materials Research, 2012, 594-597, 804-807.	0.3	0
266	An Input-Output Optimal Control Model under Uncertain Influence and its Solution. Advanced Materials Research, 2012, 433-440, 2974-2979.	0.3	0
267	Simulating ionization spectra for small biomolecules in inner and valence shells. , 2012, , .		0
268	Inheritance and correlation of nucleic acid pyrimidine bases. International Journal of Quantum Chemistry, 2013, , n/a-n/a.	1.0	0
269	Study of Mine Environment Monitoring System Based on Wireless Sensor Network. Applied Mechanics and Materials, 0, 278-280, 809-812.	0.2	0
270	Effect of Annealing Treatment on Structure and Electrochemical Properties of LaNi <sub>4.5</sub> Co <sub>0.25</sub> Al <sub>0.25</sub> Alloy with Low Co Content. Advanced Materials Research, 0, 788, 141-146.	0.3	0

#	Article	IF	CITATIONS
271	DFT Study on the Conformational and Vibrational Properties of 3'-Deoxycytidine and Its Analogues. International Journal of Chemistry, 2013, 5, .	0.3	0
272	Temperature Sensitivity Analysis of Temperature Control Parameters for Massive Concrete Mixing with Slag Powder and Fly Ash. Advanced Materials Research, 2013, 671-674, 1932-1935.	0.3	0
273	Valence orbital response to methylation of uracil. International Journal of Quantum Chemistry, 2014, 114, 314-320.	1.0	0
274	Structural and Spectroscopic Study of the Tyrosine Kinase Inhibitor PD-153035. Biophysical Journal, 2019, 116, 568a.	0.2	0
275	The electronic structure of bicyclo[2.2.2]octa-2,5-dione. Chemical Physics Letters, 2020, 757, 137877.	1.2	0
276	Cover Image, Volume 120, Issue 23. International Journal of Quantum Chemistry, 2020, 120, e26513.	1.0	0
277	Conformational Processes in L-Alanine Studied Using Dual Space Analysis. Lecture Notes in Computer Science, 2006, , 82-88.	1.0	0
278	Comparative Genomics of Pathogens. , 2010, , 73-91.		0
279	Application Of Computational Methods To The Rational Design Of Photoactive Materials For Solar Cells. , 2017, , 179-207.		0